

## Alternative splicing, muscle contraction and intraspecific variation: associations between troponin T transcripts, $\text{Ca}^{2+}$ sensitivity and the force and power output of dragonfly flight muscles during oscillatory contraction

James H. Marden\*, Gail H. Fitzhugh, Mahasweta Girgenrath, Melisande R. Wolf  
and Stefan Girgenrath

208 Mueller Laboratory, Department of Biology, Pennsylvania State University, University Park, PA 16802, USA

\*e-mail: jhm10@psu.edu

Accepted 23 July 2001

### Summary

The flight muscles of *Libellula pulchella* dragonflies contain a mixture of six alternatively spliced transcripts of a single troponin T (TnT) gene. Here, we examine how intraspecific variation in the relative abundance of different TnT transcripts affects the  $\text{Ca}^{2+}$  sensitivity of skinned muscle fibers and the performance of intact muscles during work-loop contraction regimes that approximate *in vivo* conditions during flight. The relative abundance of one TnT transcript, or the pooled relative abundance of two TnT transcripts, showed a positive correlation with a 10-fold range of variation in  $\text{Ca}^{2+}$  sensitivity of skinned fibers ( $r^2=0.77$ ,  $P<0.0001$ ) and a threefold range in peak specific force ( $r^2=0.74$ ,  $P<0.0001$ ), specific work per cycle ( $r^2=0.54$ ;  $P<0.0001$ ) and maximum specific power output ( $r^2=0.48$ ,  $P=0.0005$ ) of intact muscle. Using these results to reanalyze previously published data for wing kinematics during free flight, we show that the relative abundances of these particular transcripts are

also positively correlated with wingbeat frequency and amplitude. TnT variation alone may be responsible for these effects, or TnT variation may be a marker for changes in a suite of co-regulated molecules. Dragonflies from two ponds separated by 16 km differed significantly in both TnT transcript composition and muscle contractile performance, and within each population there are two distinct morphs that showed different maturational trajectories of TnT transcript composition and muscle contractility. Thus, there is broad intraspecific variability and a high degree of population structure for contractile performance phenotypes, TnT ribotypes and ontogenetic patterns involving these traits that affect locomotor performance.

Key words: dragonfly, insect flight muscle, work loop, skinned fiber,  $\text{Ca}^{2+}$  sensitivity, cooperativity, troponin T, alternative splicing, *Libellula pulchella*.

### Introduction

Whole-genome sequencing has revealed that the difference in gene number between unicellular eukaryotes and complex multicellular organisms is surprisingly small. The genomes of *Drosophila*, *Caenorhabditis*, *Arabidopsis* and *Homo* contain approximately  $13 \times 10^3$ ,  $18 \times 10^3$ ,  $25 \times 10^3$  and  $38 \times 10^3$  genes respectively; these values are only two- to sixfold greater than that of yeast ( $6 \times 10^3$  genes) (Szanthmary et al., 2001). Thus, one of the challenges facing contemporary biology is to determine how specialized tissues, organs and life histories have evolved and function using such a surprisingly small inflation of gene number (Powledge, 2000). One hypothesis is that alternative splicing and other modifications of gene transcripts and proteins provide the basis for increased physiological complexity (Ewing and Green, 2000). This hypothesis is supported by the observation that only three genes in yeast are alternatively spliced compared with an estimated 30–60 % of human genes (Sorek and Amitay, 2001). Understanding how ribotypic variation affects higher-level

processes is thus becoming a prominent area of research in functional genomics.

How alternative splicing of RNA affects function at the subcellular and cellular levels is becoming increasingly well understood (Baker et al., 2001; Pilotte et al., 2001), for example, as are ways in which the precise control of RNA splicing affects cell fate and organogenesis (e.g. sex determination in *Drosophila*; Lopez, 1998). Alternative splicing may be one of the primary mechanisms underlying phenotypic plasticity and acclimation yet, curiously, relationships between ribotypic variation and continuously variable organismal traits have received scant attention. It is also likely that there is heritable variation in the regulation of alternative splicing within populations, in which case the identity and evolution of alternative-splicing-regulating genes should be a topic of interest for population and evolutionary biology.

Here, we present a study that examines the relationship between ribotypic variation and a continuously variable trait

and how ribotypes and trait values differ among populations and morphs. Specifically, we relate intraspecific variation in transcript composition of the troponin T (TnT) gene with intraspecific variation in the contractile performance of dragonfly flight muscles. Dragonflies hunt, defend territories and mate aerially, and their flight muscle contractile performance is therefore likely to have a powerful effect on virtually all aspects of their adult biology and reproductive fitness.

Unlike many insects that have asynchronous, stretch-activated flight muscles (Josephson et al., 2000), dragonflies have synchronous flight muscles in which each contraction is initiated by a neural stimulus (Simmons, 1977b), with no evidence for stretch activation. Neural stimulation causes release of  $\text{Ca}^{2+}$  from the sarcoplasmic reticulum, which then binds with the troponin complex on the thin filament to initiate cross-bridge binding, an increase in tension and muscle shortening (Ohtsuki, 1999). We have shown in previous work that one of the three troponin subunits, troponin T (TnT), exists as multiple isoforms in the flight muscles of *Libellula pulchella* dragonflies, that ontogenetic variation in TnT isoform expression is correlated with changes in isometric twitch tension, whereas tetanic tension and unloaded shortening velocity are age-invariant (Fitzhugh and Marden, 1997), and that the mixture of TnT alternative transcripts is significantly related to variation in wing kinematics during free flight, which in turn affects aerial performance and the energetic cost of flight (Marden et al., 1999).

Because insect flight muscles operate at high contraction frequencies, the mediation of activation and relaxation by the troponin complex is likely to play an especially important role. At high contraction frequencies, the transition phase between activation and relaxation constitutes a high proportion of the total contraction cycle, and steady-state conditions are probably never attained. The work-loop technique (Josephson, 1985; Stevenson and Josephson, 1990) was developed for the purpose of assessing muscle contractile performance under realistic stress, strain and stimulation regimes, in which the non-steady-state characteristics of contraction can be observed and quantified. Here, we use the work-loop technique to determine how variation in the relative abundance of TnT transcripts is related to contractile function during a reasonable approximation of *in vivo* working conditions. The results contribute to our goal of developing an integrative understanding of muscle physiology and locomotor performance in this species (Marden et al., 1998) and, more generally, to knowledge of how molecular and cellular variation affect the complex *in vivo* mechanics of muscle contraction (Lutz and Lieber, 2000; Wakeling et al., 2000). We also explore ontogenetic and population differences in alternative splicing of TnT. Our findings highlight the need for population and evolutionary studies of processes that control alternative splicing, in addition to more commonly examined types of allelic variation [e.g. (Watt, 1992; Harrison et al., 1996; Powers and Schulte, 1998)].

## Materials and methods

### Animals

*Libellula pulchella* Drury dragonflies were collected from the wild in Centre and Huntingdon County, Pennsylvania, USA, during June–August 1998 and May–August 1999 at Ten Acre Pond and Mothersbaugh Pond (these ponds are separated by 16 km). After capture, they were placed immediately in an insulated cooler (10–15 °C). Dragonflies were used within a few hours or stored for up to 24 h at 17 °C.

### Tissue preparation and RNA analysis

Following completion of experiments with intact muscle (described below), approximately half the total flight musculature from each dragonfly was flash-frozen and stored in liquid nitrogen, or at –70 °C, for use in TnT isoform profiling. Additional tissue was placed in isotonic buffer solution (as described by Marden et al., 1999) with 1 % Triton X-100 and glycerol, and kept at –20 °C. This tissue was stored for up to 2 weeks prior to determination of skinned fiber  $\text{Ca}^{2+}$  sensitivity.

A fluorescent labeling technique (Luehrsen et al., 1997) was used to quantify the relative abundance of different TnT transcripts in the flight muscle of individual dragonflies (Wolf, 1999; Marden et al., 1999). RNA was recovered from muscle samples using RNeasy (Ambion, Austin, TX, USA) and reverse-transcribed to first-strand cDNA (Boehringer-Mannheim). TnT cDNAs were amplified using primers that span the alternatively spliced region. The forward primer, located in the 5' untranslated region, was fluorescently labeled with 6fam dye (5'-6fam CGCTTCTTTCACTCGTTGTTCACAAAC-3'). The reverse primer (5'-CCTTCGCTTGCTTGCTTC-3') was located in a constitutive exon downstream (3') from the alternatively spliced region. The amplified TnT fragments were separated on an ABI 377 automated sequencer (Applied Biosystems) and quantified according to the amount of fluorescence detected (GeneScan 2.1; Applied Biosystems).

We used the peak heights from the GeneScan profiles to determine the relative quantity of each TnT fragment. Our measures of transcript relative abundance show qualitative agreement with protein isoform composition determined from two-dimensional gels and western blots (Marden et al., 1999); this agrees with results from other studies that have found that the relative abundances of alternatively spliced TnT transcripts correspond closely to the abundances of the protein isoforms they encode (Mesnard-Rouiller et al., 1997). Thus, we assume that variation among individuals in relative abundance of different TnT transcripts is a reasonably accurate measure of variation in TnT protein isoforms within the flight muscles.

Relative quantities of each isoform were arcsine-transformed prior to statistical analyses (Sokal and Rohlf, 1995). All statistical analyses were performed with JMP software (SAS Institute).

### $\text{Ca}^{2+}$ sensitivity

Measurements of the  $\text{Ca}^{2+}$  sensitivity of force generation by detergent-skinned fibers were obtained as described previously

(Marden et al., 1999). These experiments began with a small fiber bundle (mean diameter 53  $\mu\text{m}$ ) completely submerged in a chamber containing isotonic relaxing solution (pCa8) at 25 °C. The bundle was held at each end with clamps similar to those described previously (Moss, 1979), one of which was attached to a three-dimensional micromanipulator and the other to a 404A force transducer (Aurora Scientific). Sarcomere lengths were set at 2.3–2.4  $\mu\text{m}$  (which matches the native sarcomere length determined by fixation of *in situ* muscle) using a Leica DMIL inverted microscope equipped with a CCD camera and monitor. Relaxing solution was replaced by activating solutions of progressively higher  $\text{Ca}^{2+}$  concentration, and isometric tension was measured after equilibration in each activating solution. The  $\text{Ca}^{2+}$  sensitivity of the fiber bundle was characterized as the negative logarithm of the  $\text{Ca}^{2+}$  concentration producing half-maximal tension (pCa<sub>50</sub>). The Hill cooperativity coefficient ( $n_{\text{H}}$ ) was determined from an iterative fit of the Hill equation.

#### Determination of the *in vivo* contractile regime

The wingbeat frequencies and amplitudes used by *L. pulchella* during high-performance free flight [upper quartiles 36 Hz and 68° for a sample of 59 escape flights; data from (Marden et al., 1999)] are also exhibited during high-effort flight attempts by dragonflies attached to a force transducer (Fig. 1B). At maximal effort, the net vertical forces over a number of wingbeat cycles by *L. pulchella* tethered in this fashion average approximately three times body weight (Marden, 1995), which corresponds with the maximal load that this species can lift during free flight (Marden, 1987). These data indicate that the contractile regime of the flight muscles during bouts of high-effort tethered flight should be a reasonably close approximation to the *in vivo* working conditions of the muscle during peak effort (excluding quick turns and maneuvers, which have different wingbeat kinematics).

We focused our study on the basalar muscle of the mesothorax (Fig. 1A) [(Snodgrass, 1935); this is muscle dvm3 in the terminology of Simmons (Simmons, 1977a; Simmons, 1977b)], which drives the downstroke of the forewing leading edge. This muscle is readily accessible and can be mechanically isolated with minimal perturbation. To determine the stimulus and strain regime of the basalar muscle during tethered flight, we used a laser distance sensor (LDS 80, DynaVision, Vancouver, Canada) in combination with electromyographic (EMG) recordings. The LDS was positioned 80 mm above the wingbase, with the laser striking a small area of white paint applied to the base of the forewing (Fig. 1C). The lens of the LDS detected changes in the position of the laser image during wing motion. Analog signals from the LDS were recorded at a sampling frequency of 1 kHz by a MacLab/8 analog-to-digital converter and a Macintosh Quadra 700 computer. Two 0.025 mm diameter stainless-steel wires, insulated except at the tips, were inserted into the basalar muscle (Fig. 1C), and a third wire placed in the abdomen served as a reference electrode. The voltage difference between

the two recording electrodes and the common reference electrode was determined by a differential amplifier (DAM 50, World Precision Instruments) and was recorded by the computer simultaneously with the signal from the LDS. As described more fully below, these simultaneous recordings of wing position and EMG activity in the muscle allowed us to determine the muscle strain regime and the phase relationship between muscle strain and stimulation.

The distance-calibrated LDS voltage waveform was used to determine the wing angle during flapping (Fig. 1D). From these data and a measurement of the distance between the insertion point of the tendon-like apodeme of the basalar muscle and the wing hinge, we calculated the strain cycle of the basalar muscle during high-exertion flight attempts. We confirmed these estimates by also positioning the laser of the LDS on the humeral plate (Snodgrass, 1935) of the forewing, directly above the insertion point of the basalar muscle's apodeme (Fig. 1A). Both methods estimated the peak-to-peak distance variation of the basalar muscle to be approximately 0.52 mm during high-amplitude flapping. This value is approximately 10 % of the resting length of the basalar muscle (mean basalar muscle length 5.4 mm).

EMG electrodes were inserted approximately 1 mm apart, midway along the length of the basalar muscle. Voltage spikes followed a slow time course (approximately 5 ms rise time; Fig. 2A) and had variable amplitudes; these features are characteristic of both intracellular and extracellular recordings from dragonfly motor neurons and flight muscles (Fig. 2B) [data from (Simmons, 1977b)], which do not fire conventional all-or-none action potentials.

Although the EMG traces are similar to the wing position traces and therefore give the appearance of being motion artifacts, various features of the EMG signals demonstrate that there was little contribution of motion artifacts: the first and last wing motions of each burst of wing flapping frequently occurred independently of variation in the EMG signal (Fig. 2A); the highest EMG amplitudes were often at frequencies too high to generate large-amplitude wing motions (Fig. 2A; these high frequencies presumably represent struggling, i.e. an artifact of being tethered); and externally imposed wing motion (and thus motion of the attached muscle) resulted in no detectable excursion of the EMG signal. We also observed occasional single, spontaneous EMG spikes in the absence of extensive wing motion. All these features, together with the fact that these were differential signals from electrodes referenced to a common ground (a technique that filters out most motion artifacts), indicate that the EMG signals were electrical events within the muscle.

The slow time course of electrical events in dragonfly flight muscles made it difficult to determine the *in vivo* phase relationship between the precise onset of stimulation and muscle strain. Thus, in preliminary work-loop experiments, we varied the stimulus onset in a series of 1 ms steps so that it occurred at seven different points on the strain cycle (Fig. 3). The stimulus phase onset that optimized net work during contraction at 37 Hz was approximately 22 % of the total strain

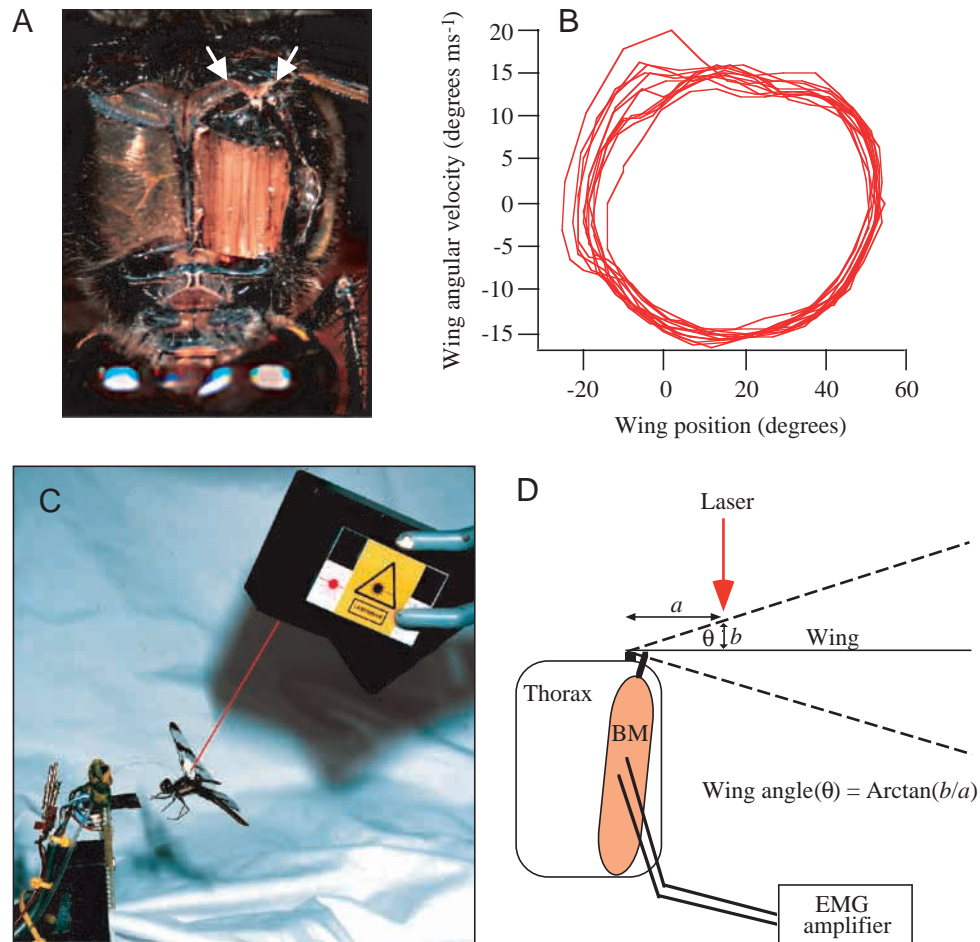


Fig. 1. (A) The basalar muscle (BM) of the mesothorax exposed by removal of a portion of the cuticle and underlying air sacs. The viewpoint is looking posteriorly from the rear margin of the head and slightly above the dragonfly; the base of the left forewing is visible near the upper right. White arrows show the lateral edges of the humeral plate, around which incisions were made to isolate the basalar muscle mechanically for studies of contractile performance. (B) Sample trace of wing position and velocity from a recording made using a laser distance sensor on the base of the forewing. (C) Photograph showing a dragonfly attached by its ventral thorax to a narrow glass beam (not visible) that extends from a strain gauge. A fine-gauge thermocouple and EMG electrodes are inserted into the thorax. The laser distance sensor is shown at the upper right. We have drawn a red line to depict the laser beam striking a white spot painted at the base of the right forewing. (D) Diagram showing the geometry of the basalar muscle attachment to the base of the forewing, an approximation of the EMG recording electrodes (these are differential electrodes referenced to a third electrode in the abdomen that is not shown) and the method used to calculate wing position from the laser distance sensor.

cycle (i.e. at 44 % of the lengthening portion of the cycle). We used this stimulus phase in subsequent experiments.

#### Contractile properties

To measure the contractile performance of the intact basalar muscle, the dragonfly's head, wings and legs were clipped, and the ventral thorax was attached with quick-setting epoxy resin to the base of a temperature-controlled chamber. The basalar muscle was isolated by making a series of small incisions around the humeral plate, which is the insertion point of the basalar apodeme (Fig. 1A). This involved minimal penetration of the exoskeleton and little or no disruption of the air sacs that surround and ventilate the flight muscles. A fine suture was tied around the top of the apodeme and was used to anchor (with cyanoacrylate glue) an insect pin suspended from the lever arm

of a Cambridge Technology 300B ergometer. Once attached to the apodeme, the pin formed a rigid mechanical linkage between the basalar muscle and the lever. The stage holding the lever system was raised or lowered, then locked in place when the muscle was held at its resting length, as judged by the position of the undisturbed contralateral humeral plate. The sarcomere lengths of muscles in this position correspond to the sarcomere lengths used in our measures of the Ca<sup>2+</sup> sensitivity of skinned fibers. Fine adjustments to the lateral position of the lever system were made so that the long axis of the muscle was aligned according to the *in vivo* position.

Muscle temperature was monitored with a fine-gauge thermocouple implanted in the center of the thorax. The contractile performance of some preparations began to degrade between initial tests at 28 °C and the target test



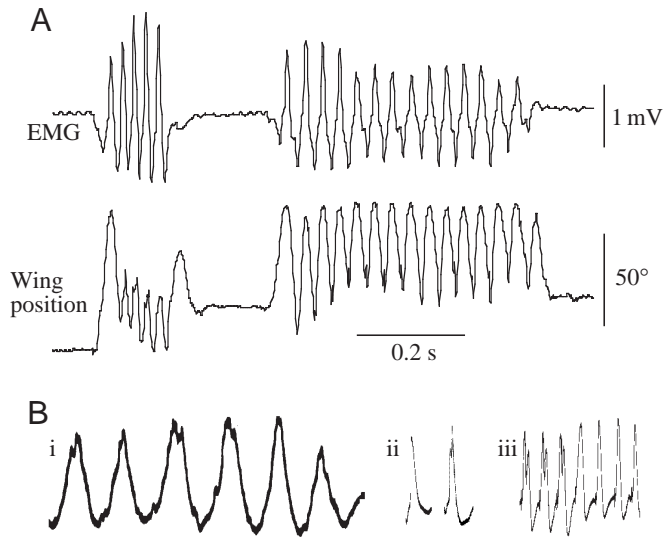


Fig. 2. (A) Simultaneous recordings from EMG signals and wing position during tethered flight (see Fig. 1C,D). Note the slow time course and variable amplitude of EMG events. The first burst of neural events had a frequency (44 Hz; this is presumably an artifact of tethered flight) that resulted in relatively little wing motion. The second burst is at a lower frequency, which resulted in a higher wingbeat amplitude and an average vertical force that was 1.87 times body weight (measured simultaneously from a strain gauge; that trace is not shown here). (B) Examples of recordings made by Simmons (Simmons, 1977b), which have been reproduced here to match the relative amplitude and time scale of the EMG traces shown in A. Simmons' data are (i) from intracellular electrodes in a flight muscle motor neuron during low-frequency wing flapping, (ii) from intracellular electrodes in a motor neuron caused to fire by peripheral electrical stimulation at the muscle and (iii) from an extracellular suction electrode attached to a small group of muscle fibers during tethered flight. Both intra- and extracellular recordings show variability in the time course and amplitude of spikes. The time base shown in A applies also to B.

temperature of 32 °C; degradation consisted of a marked increase in passive tension accompanied by a decrease in active tension. To avoid reductions in sample size, we analyzed, for each individual, the series of contractions at any temperature between 28 and 32 °C that produced the highest power output, and we included temperature as a variable in our statistical analyses. Most of the muscle preparations deteriorated rapidly at temperatures greater than 32–34 °C. Our total sample consisted of one basalar muscle from each of 21 individual dragonflies.

Analog output from a computer was used to drive the lever and the attached basalar muscle through a series of oscillations that corresponded to 10 % strain at integer frequencies from 20 to 45 Hz. The computer program (a macro written in Igor; Wavemetrics Inc.) triggered a single electrical stimulus of 0.25 ms duration (determined in preliminary experiments to be the minimal stimulus duration required to evoke maximal twitch tension). Five contraction cycles were measured at each frequency; we analyzed the fourth cycle from each of these sets. At each frequency, we also recorded tension during a strain cycle that lacked a stimulus; the resulting trace of passive tension was overlaid on the trace of active tension at that frequency to determine the time of onset of active force.

Net work output was measured from the area enclosed by counterclockwise-progressing work loops, minus any area within clockwise-progressing portions (i.e. the product of net force and distance) (Josephson, 1985); the product of net work and frequency yielded mechanical power output. To quantify variability in the shape of work loops, we measured the following variables at several contraction frequencies (20, 24, 27, 30, 34, 37, 40 and 44 Hz): the time of onset of active force, peak force, force at 50 % of the shortening phase and the time from 50 % of peak activation to 50 % relaxation (i.e. half-width of activation). Fig. 4 illustrates these variables. For measures involving only the magnitude of forces, we have normalized

Table 1. *Fragment sizes and mean relative abundances of the PCR products obtained from amplification of the 5' alternatively spliced region of Libellula pulchella TnT cDNA*

cDNA fragment size (number of base pairs)	Deduced amino acid sequence of variable region	Mean relative abundance (% of total TnT transcripts)
243	MSDEEEYSEEEEEV.....	4.5±3.8 (0–10.4)
246	MSDEEEYSEEEEEV.....K.....	9.9±10.4 (0–42.0)
258	MSDEEEYSEEEEEV.....RPRGK.....	53.4±14.7 (35.9–82.1)
261	MSDEEEYSEEEEEV.....K.....RPRGK.....	26.8±12.9 (0–47.4)
267	MSDEEEYSEEEEEV.....KEPEKKTE.....	4.7±4.0 (0–13.3)
270	MSDEEEYSEEEEEV.....K.....KEPEKKTE.....	0.3±0.8 (0–2.7)
285	MSDEEEYSEEEEEV.....K.....KEPEKKTE.....RPRGK.....	Not in flight muscle
Exon	2/3      4      5      6	

Values of abundance are means ± S.D. (range) (N=21).

Note that these values are the raw data prior to the arcsine transformation that was used for all statistical analyses and figures.

Also shown are the deduced amino acid sequences from characterized cDNAs that correspond to the 5' variable region of these fragments. Exons are separated by gaps. Constitutive exon 7 (not shown) begins after the 3'-most base shown for each sequence.

A fragment (285 base pairs) present in other *L. pulchella* muscles (Wolf, 1999) is not found in flight muscle but is shown here to illustrate a transcript that contains all three variable exons.

for a small amount of variation in resting tension (mean  $0.6\text{ N cm}^{-2}$ ) by subtracting the minimum force measured for each cycle from the active forces; the reported force measurements are therefore net forces.

At the end of the contractile measurements, muscle length was measured *in situ*, and the muscle was removed from the

experimental apparatus and weighed. This procedure took less than 1 min, with minimal dehydration of the muscle during dissection and weighing. The cross-sectional area was estimated from the ratio of muscle mass to length.

Results

TnT transcripts

Six different cDNAs of TnT, which differ near their 5' end, were identified from flight muscles of *L. pulchella* (Table 1). The pattern of variation among these cDNAs is entirely consistent with alternative splicing of exons 4, 5 and 6 of the single-copy *L. pulchella* TnT gene (S. Girgenrath and J. H. Marden, in preparation). We have sequenced a seventh cDNA that does not occur in flight muscle, and a polymerase chain reaction (PCR) fragment of 282 base pairs (presumably containing exons 5 and 6, without exon 4) was present on some of our gels but not in any of our sequenced subclones (Wolf, 1999). Thus, it appears that all eight possible combinations of the three variable exons are produced but that one is expressed in a tissue-specific manner (fragment 285) and another is very rare (fragment 282).

Contractile performance at the cellular level: thin filament activation by  $\text{Ca}^{2+}$

Skinned fibers from different individuals showed wide variation in  $\text{Ca}^{2+}$  sensitivity ( $\text{pCa}_{50}$ ) and cooperativity of thin filament activation (characterized by the Hill coefficient,  $n_H$ ). Fig. 5 shows data from fibers that represent the high and low extremes of  $\text{Ca}^{2+}$  sensitivity (Fig. 5A) and from fibers that have approximately the same  $\text{Ca}^{2+}$  sensitivity but very different Hill coefficients (Fig. 5B). As suggested by Fig. 5, these two parameters varied independently of each other ( $r^2=0.04$ ,  $P=0.17$ ,  $N=52$ ).  $\text{Ca}^{2+}$  sensitivity varied as much as 10-fold among individuals, and a substantial proportion of the variation was explained by the pooled relative abundance of

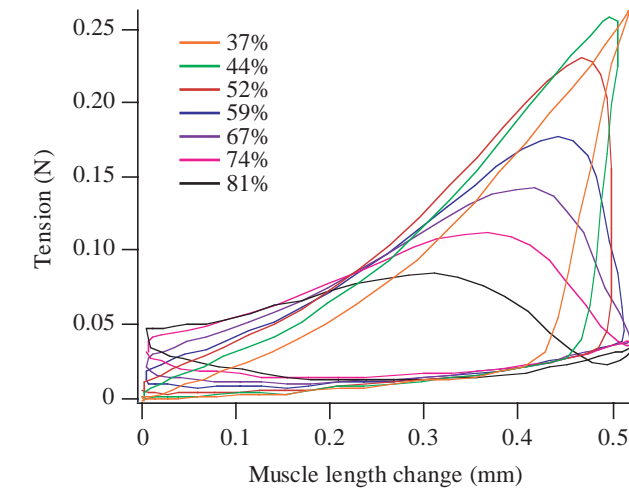


Fig. 3. Work loops at a contraction frequency of 37 Hz for a muscle preparation stimulated at seven different points on the strain cycle. Net work output was maximized in the green trace, which was produced by stimulation at 44 % of the lengthening cycle. The phase (percentage of the lengthening cycle) for the other stimulus phase relationships tested are shown.

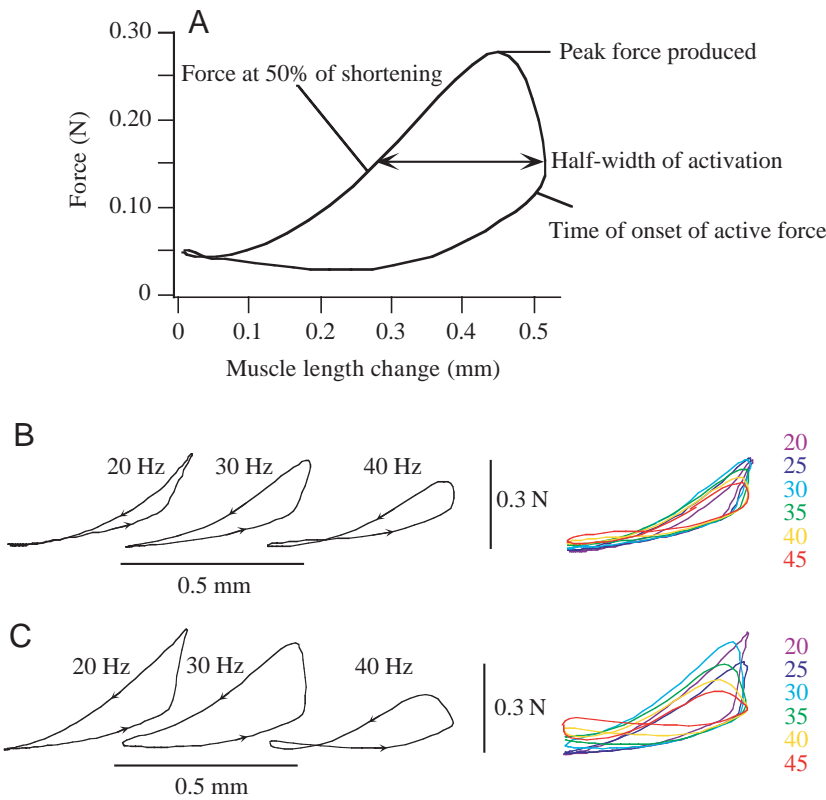


Fig. 4. (A) Work loop from a basalar muscle contracting at 37 Hz and an illustration of the variables measured for work-loop analyses. (B,C) Work loops at various contraction frequencies for two basalar muscles that represent the range of variation in specific work and power output. Force is plotted as a function of changes in muscle length. Arrowheads indicate the direction of progression around the loop. The muscle in B was larger (16.7 mg), yet generated less tension and power (maximum power at any frequency was  $66\text{ W kg}^{-1}$ ) than the muscle in C (14.8 mg;  $156\text{ W kg}^{-1}$ ). Both series were obtained at a tissue temperature of  $32^\circ\text{C}$  and a constant phase between electrical stimulation and muscle lengthening. Net work is as follows: B,  $0.9\text{ J kg}^{-1}$  for 20 Hz,  $2.1\text{ J kg}^{-1}$  for 30 Hz and  $1.3\text{ J kg}^{-1}$  for 40 Hz; C,  $3.7\text{ J kg}^{-1}$  for 20 Hz,  $5.0\text{ J kg}^{-1}$  for 20 Hz and  $2.3\text{ J kg}^{-1}$  for 20 Hz.

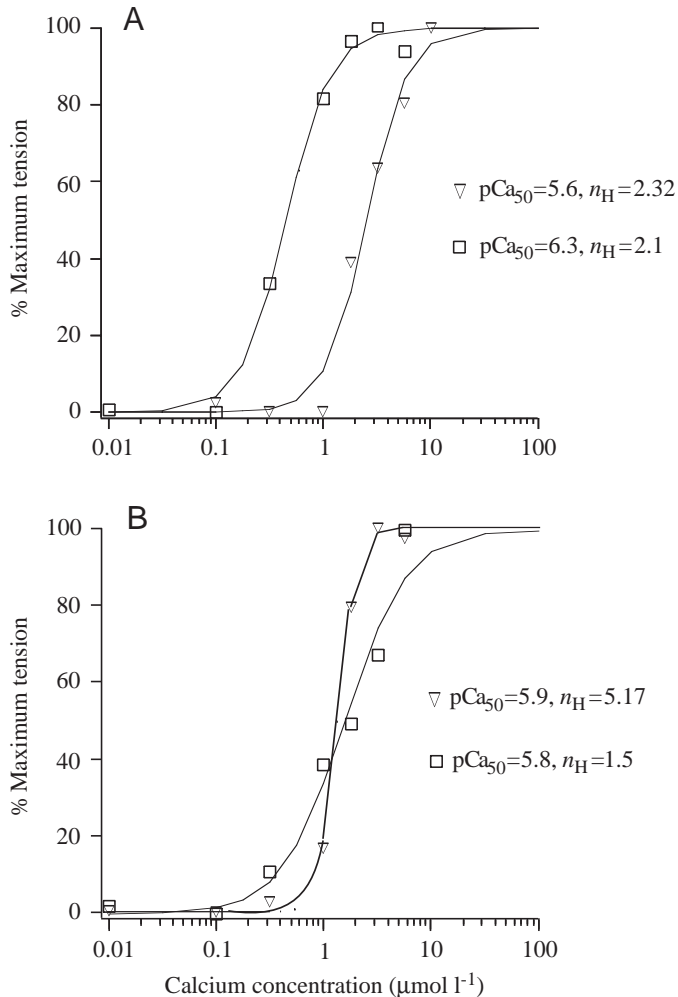


Fig. 5. Examples of the  $\text{Ca}^{2+}$  concentration/tension relationship measured from different skinned muscle fiber preparations. Tension is expressed as a percentage of maximum tension. (A) Muscle fibers with different  $\text{Ca}^{2+}$  sensitivity ( $\text{pCa}_{50}$ ) and similar Hill coefficients ( $n_H$ ). (B) Muscle fibers with similar  $\text{Ca}^{2+}$  sensitivity but different Hill coefficients.

TnT 261 and 267 ( $r^2=0.77$ ,  $P<0.0001$ , Fig. 6). There were no significant relationships between the relative abundance of any TnT transcript and the Hill coefficient.

#### Differences among morphs in the maturational pattern of $\text{Ca}^{2+}$ sensitivity

At both our study ponds, there are two morphs of *L. pulchella* dragonflies that differ in size, seasonal timing of emergence and flight physiology (Marden et al., 1999). The early morph is present from late May to mid-July and has forewing lengths of 38–42 mm. The late morph is present from early July to late August and has forewing lengths of 42–47 mm.

Both morphs undergo a two- to threefold increase in body mass during adult maturation. This mass increase consists primarily of internal growth of flight muscle and ovaries (Marden, 1989). The extent of maturation for an individual can be quantified by relating body mass to a maturationally

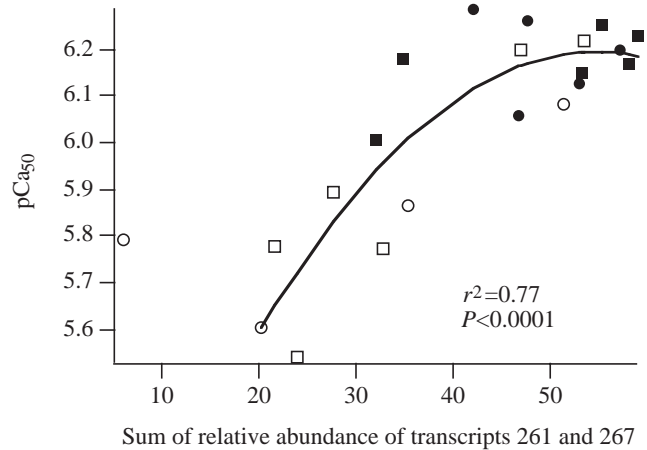


Fig. 6.  $\text{Ca}^{2+}$  sensitivity ( $\text{pCa}_{50}$ ) as a function of the sum of the relative abundance of two troponin transcripts, troponin T (TnT) 261 and TnT 267 (see Table 1). Open symbols represent individuals from Ten Acre Pond and filled symbols represent individuals from Mothersbaugh Pond. Circles represent the early-emerging morph; squares represent the late-emerging morph. The point at the far left side of the plot was excluded from the statistical analysis and the curve fit because it does not conform to either linear or curvilinear models. It does, however, support the association between low levels of particular TnT transcripts and low  $\text{Ca}^{2+}$  sensitivity.

invariant exoskeletal dimension. For this purpose, we use residuals from the regression of the cube root of body mass on forewing length as an index of relative maturity. Dragonflies belonging to the early morph showed a significant relationship between relative maturity and the  $\text{Ca}^{2+}$  sensitivity of muscle activation (Fig. 7A;  $r^2=0.64$ ,  $P<0.0001$ ), whereas the late morph showed no such relationship (Fig. 7B;  $r^2=0.0002$ ,  $P=0.85$ ). The relative abundance of TnT 267 also increased significantly with relative maturity in the early morph ( $r^2=0.26$ ,  $P=0.02$ ) but not in the late morph ( $r^2=0.17$ ,  $P=0.10$ ), whereas the relative abundance of TnT 261 increased significantly with relative maturity in both morphs ( $r^2>0.4$ ,  $P<0.004$  in both morphs). Thus, distinct subpopulations follow different ontogenetic trajectories for certain aspects of alternative splicing and muscle contractile physiology.

#### Contractile performance of intact muscle: work-loop analyses

We analyzed the work-loop characteristics of intact muscles across a wide range of contraction frequencies, but the differences in contractile performance among individuals were quite consistent across all frequencies (Fig. 4B,C). Thus, to avoid redundancy and inflation of the number of independent data points, we report below only our results from contractions at 37 Hz, a frequency that was chosen *a priori* because it corresponds to a typical wingbeat frequency for mature *L. pulchella* dragonflies during free flight (Marden et al., 1999). Almost without exception, the significant relationships we show for 37 Hz are true for other frequencies as well.

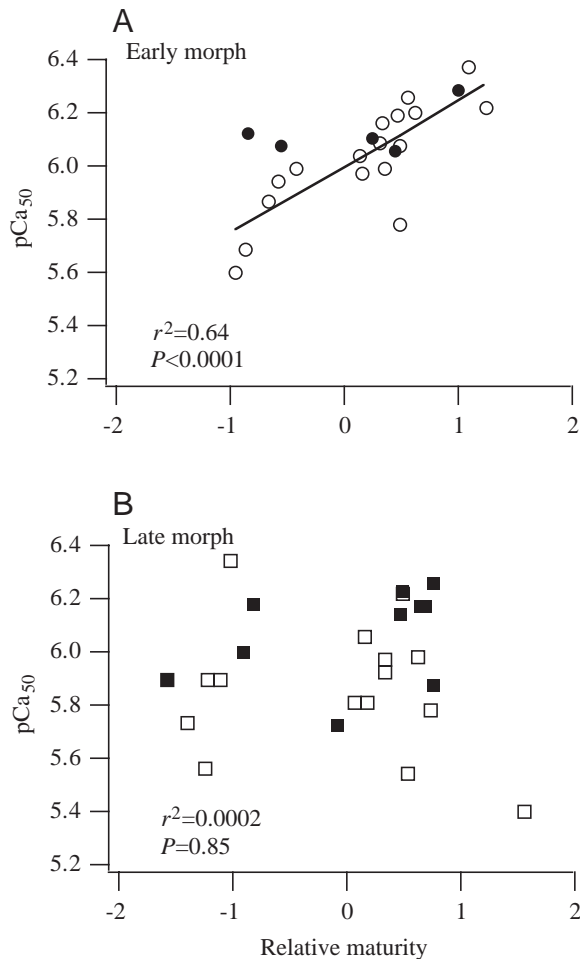


Fig. 7.  $\text{Ca}^{2+}$  sensitivity ( $\text{pCa}_{50}$ ) as a function of relative maturity, measured as residuals of the regression of the cube root of body mass on forewing length. (A) Data representing the early-emerging morph. (B) Data representing the late-emerging morph. In both panels, open symbols represent individuals from Ten Acre Pond; filled symbols represent individuals from Mothersbaugh Pond.

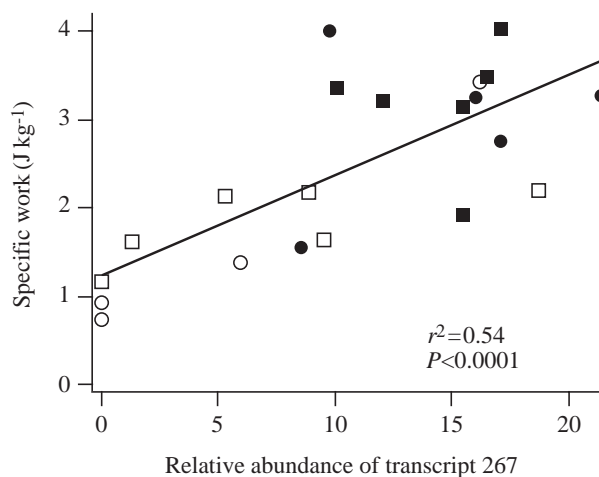


Fig. 8. Specific work ( $\text{J kg}^{-1}$ ) during work-loop contractions at 37 Hz in relation to the relative abundance of troponin T (TnT) 267. Symbols are as in Fig. 6.

#### Work per cycle

Work output at 37 Hz averaged  $2.4 \text{ J kg}^{-1}$ , with a range of  $0.73\text{--}4.0 \text{ J kg}^{-1}$ . In univariate models, specific work was positively related to the relative abundance of TnT 267 ( $r^2=0.54$ ;  $P<0.0001$ ; Fig. 8) and to  $\text{Ca}^{2+}$  sensitivity ( $r^2=0.45$ ;  $P=0.0005$ ). Neither of these relationships varied among morphs ( $P>0.74$  in both cases). In a stepwise regression analysis that included  $\text{Ca}^{2+}$  sensitivity, the relative abundance of TnT 267, the relative abundance of TnT 261, temperature, morph and the Hill coefficient (log-transformed to achieve normality) as independent variables, only the relative abundance of TnT 267 (partial  $r^2=0.53$ ;  $P=0.0004$ ) and temperature (partial  $r^2=0.09$ ;  $P=0.07$ ) had significant or marginally significant effects on specific work.

#### Timing of force production

Our experiments were performed over a narrow range of muscle temperatures ( $28\text{--}32^\circ\text{C}$ ), but nonetheless there was a detectable effect of temperature on certain aspects of work-loop shape. In bivariate regressions that included temperature and either  $\text{Ca}^{2+}$  sensitivity or the relative abundance of TnT 267, both independent variables showed weak effects on the time of onset of active force production. This onset occurred earlier at higher temperatures (partial  $r^2=0.17$  or  $0.19$ ,  $P=0.03$  in both models) and at higher levels of  $\text{Ca}^{2+}$  sensitivity (partial  $r^2=0.23$ ,  $P=0.03$ ; Fig. 9) or relative abundance of TnT 267 ( $r^2=0.17$ ,  $P=0.05$ ). A multivariate regression that used temperature,  $\text{Ca}^{2+}$  sensitivity and the relative abundance of TnT 267 as independent variables did not show a significant independent effect of either of the latter two variables. Thus,

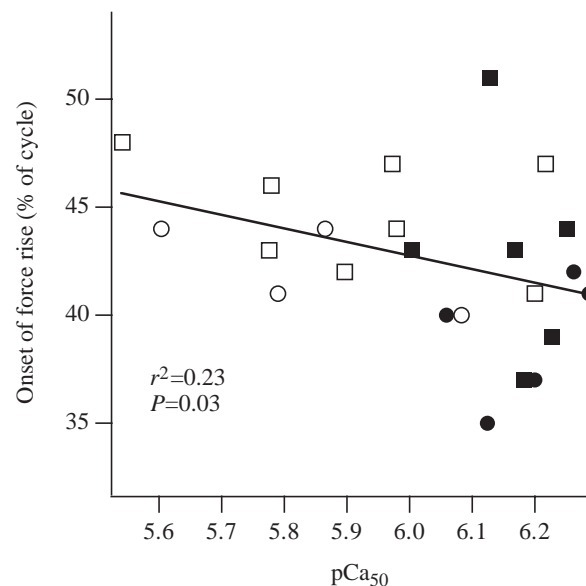


Fig. 9. Onset of active tension (shown as a percentage of the total length cycle, where 50% is the transition from lengthening to shortening; onset was judged by comparing passive with active loops for each muscle) during contraction at 37 Hz in relation to  $\text{Ca}^{2+}$  sensitivity ( $\text{pCa}_{50}$ ).



we are unable to distinguish a difference between the effect of  $\text{Ca}^{2+}$  sensitivity and TnT composition.

Neither TnT 261 nor the Hill coefficient showed a significant effect on the onset of force rise in any univariate or multivariate models.

The same set of independent variables, either alone or in multivariate combinations, failed to explain a significant proportion of the variation in the location of peak force or the half-width of activation (percentage of the contraction cycle over which force was at least 50 % of maximal). In general, these results show little effect of the measured variables on the timing of muscle activation and deactivation (although temperature certainly has a large effect when varied over a larger range).

#### Magnitude of force production

The peak net force developed during work-loop contractions at 37 Hz varied between 3.0 and 11.0  $\text{N cm}^{-2}$ .  $\text{Ca}^{2+}$  sensitivity ( $r^2=0.53$ ,  $P<0.0001$ ) and the relative abundances of both TnT 261 ( $r^2=0.42$ ,  $P=0.002$ ) and TnT 267 ( $r^2=0.35$ ,  $P=0.005$ ) each showed strong positive relationships with peak net force in univariate linear regressions. However, these are not independent effects since these variables were significantly correlated with each other. Only the relative abundance of TnT 261 had a significant effect when all three of these variables were included in a single linear model. The model that appears to best describe the variation in peak force is a quadratic fit based on the pooled relative abundance of TnT 261 and TnT 267 ( $r^2=0.74$ ,  $P=0.0001$ ; Fig. 10). The significant second-order term in this relationship ( $P=0.0003$ ) suggests that the highest observed levels of these generally force-enhancing TnT isoforms are associated with a decline in force production.

We also measured (Fig. 4) the force produced midway

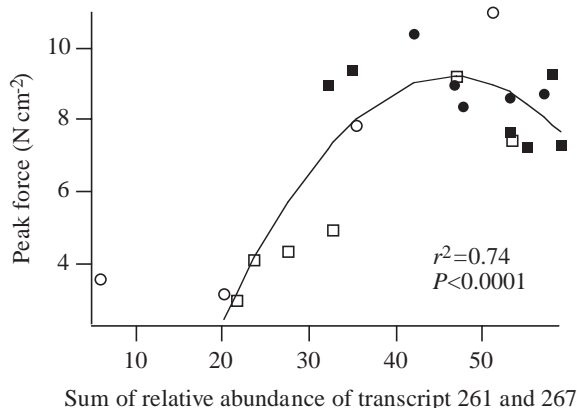


Fig. 10. Peak force produced during contraction cycles at 37 Hz in relation to the sum of the relative abundance of troponin T (TnT) transcripts 261 and 267. Symbols are as in Fig. 6. The point at the far left of the plot was excluded from the statistical analysis and the curve fit because it does not conform to either linear or curvilinear models. It does, however, support the association between low levels of particular TnT transcripts and force output.

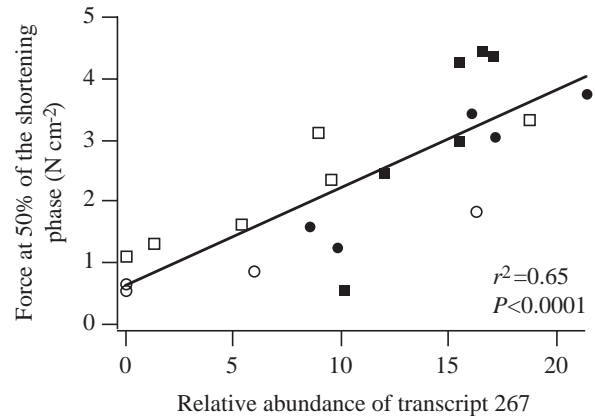


Fig. 11. Force halfway through the shortening cycle during contractions at 37 Hz in relation to the relative abundance of troponin T (TnT) transcript 267. Symbols are as in Fig. 6.

through the shortening phase of the contraction cycle. Force per cross-sectional area at this point showed a strong positive relationship with the relative abundance of TnT 267 ( $r^2=0.65$ ,  $P<0.0001$ ; Fig. 11), with little apparent effect of the relative abundance of TnT 261 (partial  $r^2=0.04$ ;  $P=0.19$ ) or  $\text{Ca}^{2+}$  sensitivity (partial  $r^2=0.01$ ;  $P=0.75$ ). Thus, in addition to the tendency for muscles with high relative quantities of TnT 261 and TnT 267 to generate a high peak force, muscles with high relative amounts of TnT 267 maintained a relatively high force during shortening. This result suggests that particular TnT isoforms affect both the magnitude of activation and the rate of shortening deactivation.

Up to this point, we have avoided redundancy by presenting only the effects of TnT 261 and TnT 267. Increases in the relative abundance of these two transcripts are correlated with decreases in the relative abundance of other TnTs, particularly TnT 258 (the other TnT transcripts are rare and show no strong relationships with any contractile variables). Thus, TnT 261 and TnT 267 may have positive effects on contractility, TnT 258 may have negative effects, or both. In general, we found greater statistical support for positive effects of TnT 261 and TnT 267 than for negative effects of TnT 258. For example, the relative abundance of TnT 258 explained only 15 % of the variation in specific work per cycle ( $P=0.07$ ) and 26 % of the variation in specific force midway through the shortening cycle ( $P=0.01$ ), and in neither of these analyses did TnT 258 have a significant effect in a multivariate model that included either TnT 267 or TnT 261 as independent variables.

#### Power output

There was a wide range of variation among individual muscles in their maximum specific power output (the highest power output recorded across all contraction frequencies; 45–155  $\text{W kg}^{-1}$ ; Fig. 12, Fig. 13). As we found for peak work-loop force, a large proportion of this variation was explained in univariate models both by the pooled relative abundance of TnT 261 and TnT 267 ( $r^2=0.48$ ,  $P=0.0005$ ; Fig. 13A) and by  $\text{Ca}^{2+}$  sensitivity ( $r^2=0.51$ ,  $P=0.0001$ ; Fig. 13B). Using both

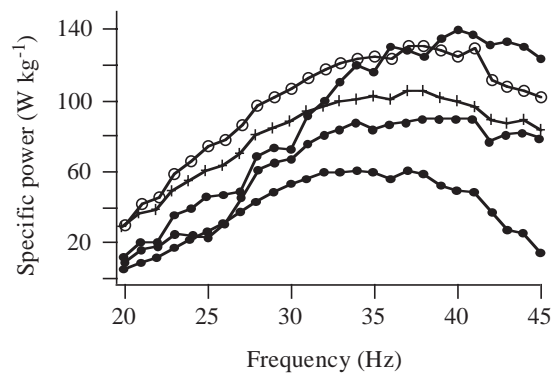


Fig. 12. Representative traces of specific power output over integer contraction frequencies between 20 and 45 Hz for five basalar muscle preparations.

Table 2. Comparison of the biochemical and contractile performance of flight muscles of <i>Libellula pulchella</i> dragonflies from two study ponds separated by 16 km				
	Pond		$r^2$	$P$
	Ten Acre	Mothersbaugh		
Tnt 261 and TnT 267	0.32±0.04	0.49±0.04	0.34	0.0005
pCa <sub>50</sub>	5.9±0.05	6.2±0.05	0.49	0.0006
Peak force at 37 Hz (N cm <sup>-2</sup> )	5.9±0.6	8.6±0.6	0.31	0.004
Specific work at 37 Hz (J kg <sup>-1</sup> )	1.7±0.2	3.1±0.2	0.43	0.005
Maximum power output (W kg <sup>-1</sup> )	91±9	124±9	0.24	0.02

Values are means ± S.E.M.,  $N=10$  for the Ten Acre Pond and 11 for Mothersbaugh Pond.

The  $r^2$  value shows the proportion of total variation explained by 'pond';  $P$  shows the type I error probability for the comparison between the means.

TnT 261 and TnT 267 refer to the sum of the relative frequency of these two transcripts in the total pool of amplified TnT transcripts.

these independent variables in a multivariate model resulted in essentially no increase in explanatory power ( $r^2=0.55$ ) and, although the overall model was highly significant, neither of these independent variables showed a significant effect independently of the other. Thus, one or both of these independent variables are correlated with maximum power output, and our data do not distinguish any differences in their effects.

Power output increased significantly with relative maturity in the early morph ( $r^2=0.59$ ,  $P<0.002$ ), but showed no relationship to relative maturity in the late morph ( $r^2=0.001$ ,  $P=0.9$ ). Relative maturity showed no relationship with power output ( $P=0.36$ ) when included together with TnT 261 and TnT 267 in a multivariate model (nor was there a significant interaction between these two independent variables).

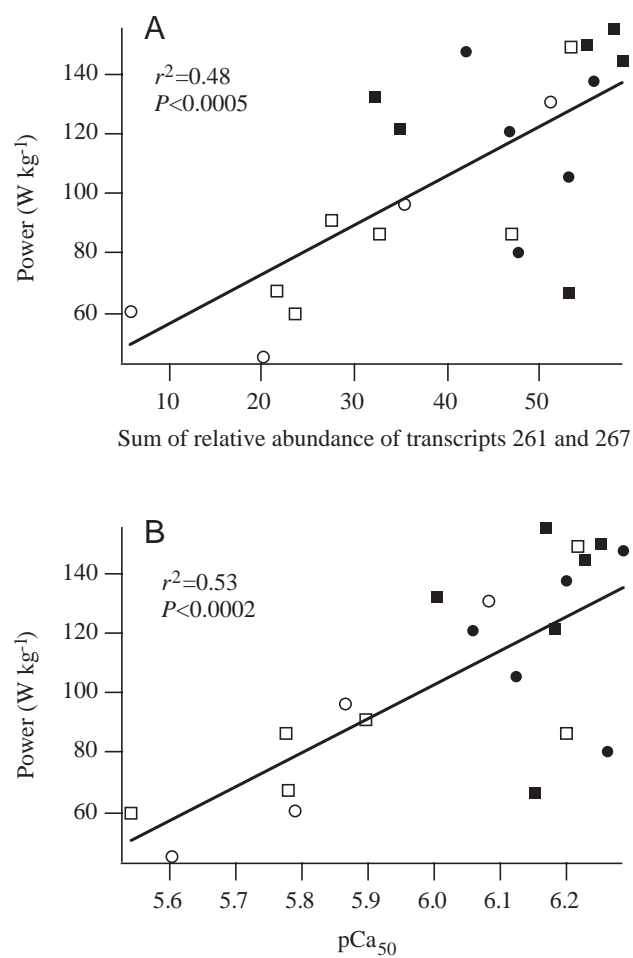


Fig. 13. (A) Maximum power output at any contraction frequency in relation to the relative abundance of troponin T (TnT) transcripts 261 and 267. (B) Maximum power output at any contraction frequency in relation to  $\text{Ca}^{2+}$  sensitivity ( $\text{pCa}_{50}$ ). Symbols are as in Fig. 6.

Optimum cycle frequency

Temperature had a weak effect on the optimal frequency for power output (i.e. the contraction frequency at which maximum power was produced;  $r^2=0.28$ ,  $P=0.01$ ); this effect becomes much more pronounced when temperature is varied over a wider range than we used in the present experiments.  $\text{Ca}^{2+}$  sensitivity, the Hill coefficient and the individual or pooled relative abundance of any TnT transcripts did not explain any of the remaining variation in optimal frequency. This result is consistent with our observation (see above) that the independent variables examined in this study had little effect on the timing of muscle activation.

Differences in contractile performance between populations

In addition to the physiological differences that we observed among morphs (Fig. 7), there were significant differences in the mean values from our two study ponds for nearly every biochemical and physiological variable that we measured (Table 2). Our data also suggest that there may be population differences in some of the relationships between

	2	3	4	6	7
	ATGTCGGACGAGGAGGAGTACTCTGAGGAGGAGGAGGTGAAGCGACCTCGCGGAAAGGGAGAAAAGGGA				
TenA.148.1	ATGTCGGACGAGGAGGAGTACTCTGAGGAGGAGGAGGAGGT---GCGACCTCGCGGAAAGGGAGAAAAGGGA				
TenA.148.2	ATGTCGGACGAGGAGGAGTACTCTGAGGAGGAGGAGGAGGT---GCGACCTCGCGGAAAGGGAGAAAAGGGA				
TenA.148.3	ATGTCGGACGAGGAGGAGTACTCTGAGGAGGAGGAGGAGGTGAA-----GGGAGAAAAGGGA				
TenA.148.4	ATGTCGGACGAGGAGGAGTACTCTGAGGAGGAGGAGGAGGT---GCGACCTCGCGGAAAGGGAGAAAAGGGA				
TenA.133.1	ATGTCGGACGAGGAGGAGTACTCTGAGGAGGAGGAGGAGGT---GCGACCTCGCGGAAAGGGAGAAAAGGGA				
TenA.133.3	ATGTCGGACGAGGAGGAGTACTCTGAGGAGGAGGAGGAGGTGAA-----GGGAGAAAAGGGA				
TenA.156.3	ATGTCGGACGAGGAGGAGTACTCTGAGGAGGAGGAGGAGGT---GCGACCTCGCGGAAAGGGAGAAAAGGGA				
Mb.11.1	ATGTCGGACGAGGAGGAGTACTCTGAGGAGGAGGAGGAGGT-----GGGAGAAAAGGGA				
Mb.11.2	ATGTCGGACGAGGAGGAGTACTCTGAGGAGGAGGAGGAGGTGAAGCGACCTCGCGGAAAGGGAGAAAAGGGA				
Mb.11.3	ATGTCGGACGAGGAGGAGTACTCTGAGGAGGAGGAGGAGGT---GCGACCTCGCGGAAAGGGAGAAAAGGGA				
Mb.11.4	ATGTCGGACGAGGAGGAGTACTCTGAGGAGGAGGAGGAGGT---GCGACCTCGCGGAAAGGGAGAAAAGGGA				
Mb.16.1	ATGTCGGACGAGGAGGAGTACTCTGAGGAGGAGGAGGAGGT---GCGACCTCGCGGAAAGGGAGAAAAGGGA				
Mb.16.2	ATGTCGGACGAGGAGGAGTACTCTGAGGAGGAGGAGGAGGT---GCGACCTCGCGGAAAGGGAGAAAAGGGA				

Fig. 14. cDNA sequence of the 5' ends of a sample of troponin T (TnT) transcripts that do not contain alternative exon 5. cDNA was amplified from three individuals from Ten Acre Pond (TenA.148, TenA.133 and TenA.156) and two from Mothersbaugh Pond (MbB.11 and Mb.16) using primers against the 5' untranslated region and constitutive exon 8. Products from polymerase chain reactions were subcloned and sequenced. The bar at the top of the plot shows the exon structure, below which is the consensus sequence. Only the coding region through a portion of exon 7 is shown here.

physiological variables. For example, the quadratic fit that we show in Fig. 10 may hide what is actually a positive linear relationship between the relative abundance of TnT 261 and TnT 267 and force production in the Ten Acre Pond population and a negative linear relationship or no relationship between these variables in the Mothersbaugh population. For most of our data, there is a relatively small range of variation for the independent variable within the Mothersbaugh population, which makes it difficult to determine whether this population shows a different relationship or simply presents too little statistical leverage to detect the trend. Without more data showing the effects of low levels of  $\text{Ca}^{2+}$  sensitivity or the relative abundance of TnT 261 in the Mothersbaugh population, it is impossible to resolve this question. The only exception to this problem is the relative abundance of TnT 267, which had a nearly equal range of variation in the two populations; here, we see an identical relationship in both populations (Fig. 8, Fig. 11).

The possibility that our two study populations have different relationships between TnT transcript levels and certain measures of muscle function stimulated us to look for allelic differences in TnT between the two populations. One intriguing hypothesis was that there might be an allelic difference within the alternatively spliced exons 4 or 6, which are present in TnT 261 but are absent from TnT 267 (Table 1). Such an allelic difference might explain why TnT 261 has little apparent effect on maximum force in the Mothersbaugh population (data not shown, but very similar to Fig. 10), whereas the effect of TnT 267 on force midway through the shortening phase was consistent across both populations (Fig. 11). To test this hypothesis, we cloned and sequenced cDNA from a subset of dragonflies from each of our study sites (Fig. 14). There were no allelic differences between any of these clones, either within or outside the alternatively spliced region. Thus, we can reject the hypothesis that the possible population differences in muscle contractile physiology are caused by allelic differences in TnT.

## Discussion

Alternative splicing of RNA creates variation in troponin T transcripts that is related to variation in subcellular and whole-muscle measures of contractile performance in the flight muscles of *L. pulchella* dragonflies. We have previously reported relationships between TnT transcript composition, wingbeat kinematics and whole-organism flight performance (Marden et al., 1999). Together with results of the present study, these data suggest that alternative splicing of a single gene may be responsible for a fairly large proportion of the variation in contractile traits at the cellular, tissue and whole-organism levels. We do not yet know whether alternative splicing of TnT is the only molecular change causing these effects or whether changes in TnT splicing are co-regulated with a suite of other molecular changes. Co-regulation of alternative expression of TnT and tropomyosin has been demonstrated in rabbit skeletal muscle (Briggs et al., 1990), so it is plausible that TnT variability in dragonflies is accompanied by changes in other contractile and regulatory proteins that together cause the observed changes in contractile performance.

Two features of our correlative results strengthen the likelihood that TnT variation has a causal role in these relationships. First, the two distinct morphs of *L. pulchella* undergo different ontogenetic patterns of  $\text{Ca}^{2+}$  sensitivity, power output and the relative abundance of one particular TnT transcript, yet these morphs are indistinguishable in all comparisons involving the relationship between TnT transcript abundances and physiological variables. Thus, we can reject the hypothesis that changes in TnT splicing are simply a marker for physiological changes related to age or maturation. Second, we found a strong relationship between the relative abundance of a particular TnT transcript (267) and a particular aspect of contraction (force per cross-sectional area midway through the shortening phase; Fig. 11). The relative abundance of TnT 267 is correlated with that of other TnT transcripts as well as with  $\text{Ca}^{2+}$  sensitivity, yet none of these other variables shows nearly as strong a relationship with force midway through the shortening phase.

A number of experimental manipulations of TnT have produced results that demonstrate a strong effect of TnT variation on muscle contractile performance. Changing TnT content, most commonly by introduction of a transgene carrying a point mutation, has been shown to cause changes in  $\text{Ca}^{2+}$  sensitivity, force and cross-bridge cycling rates in single filaments, actomyosin solutions and cultured muscle cells (Tobacman and Lee, 1987; Sweeney et al., 1998; Watkins et al., 1996; Chandra et al., 1999; Nakaura et al., 1999; Purcell et al., 1999; Rust et al., 1999; Homsher et al., 2000). One study has shown that the ratio of mutant to wild-type troponin T protein has strong effects on contractility (Redwood et al., 2000); this result is quite similar to what we found for the ratio of naturally occurring alternative transcripts. Transgenic mice carrying mutant forms of cardiac TnT have consistently shown changes in systolic and/or diastolic function of their intact hearts, as well as changes in  $\text{Ca}^{2+}$  sensitivity of cardiac skinned fibers (Oberst et al., 1998; Tardiff et al., 1999; Frey et al., 2000; Knollmann et al., 2001; Miller et al., 2001). Generally, transgenic experiments have found that mutated forms of TnT cause an increase in  $\text{Ca}^{2+}$  sensitivity, force and cross-bridge cycling rates, i.e. the mutation has disrupted the normal modulatory effect of TnT on muscle contractility.

The transgenic studies discussed above have used point mutations that cause amino acid replacements at regions of the molecule that are not affected by alternative splicing. Experimental manipulations of TnT have not yet begun to examine the functional effects of variability in TnT that arise from ubiquitous alternative splicing at the 5' end of the molecule. The study that comes closest is that of Chandra et al. (Chandra et al., 1999), who replaced native TnT with an amino-terminal truncated version of TnT (TnT-trunc). TnT-trunc interacted more strongly with tropomyosin, which stabilized contractile filaments in a submaximally activated state. That result demonstrates that the amino terminal of TnT serves to weaken the binding affinity between TnT and tropomyosin, and thereby reduces the inhibition of myosin cross-bridge attachment [for a similar result, see (Ogut and Jin, 2000)]. Thus, the strong relationship between the abundance of TnT transcripts and muscle activation and force production in dragonflies is presumably caused, at least in part, by differences in the way TnT protein isoforms affect the troponin/tropomyosin interaction that regulates muscle activation. Although our correlative data leave open the possibility that other molecular changes are involved, the studies cited above indicate that TnT alone is capable of causing the observed effects. If so, then variation in the ratio of alternatively spliced TnT isoforms may be a particularly potent mechanism for varying contractile mechanics, since small changes in the relative abundance of a fairly rare transcript, TnT 267, are associated with large changes in contractile performance.

A key mechanistic question is how variation in muscle contractile performance affects wingbeat kinematics and flight performance. Wakeling and Ellington (Wakeling and Ellington, 1997a; Wakeling and Ellington, 1997b) have performed detailed studies of wingbeat kinematics of a

libellulid dragonfly and found that the stroke plane is rigidly fixed at  $48^\circ$  from the longitudinal body axis and that variation in only two variables, wingbeat amplitude and frequency, explained more than 90% of a 4.5-fold range of variation ( $35\text{--}156\text{ W kg}^{-1}$ ) in their calculation of muscle mass-specific aerodynamic power output (we obtained this result by combining data from their two papers). In a separate study (Marden et al., 1999), we have shown that the TnT transcript mixture (expressed as the first principal component of variability among the relative abundances of all TnT transcripts) is significantly related to the wingbeat frequency of *L. pulchella* dragonflies during free flight.

Our current results allow us to reanalyze those data in a more specific fashion, since we now know that particular TnT transcripts are strongly associated with contractile performance. This reanalysis shows that the relative abundance of both TnT 261 ( $P=0.03$ , one-tailed) and TnT 267 ( $P=0.008$ , one-tailed) is positively correlated with wingbeat frequency, and that the relative abundance of TnT 261 is positively correlated with wingbeat amplitude ( $P=0.04$ , one-tailed). Thus, dragonflies with enhanced muscle contractility appear to increase the amplitude and frequency of their wingbeats. This is somewhat at odds with the results of our contractile experiments, in which our data explained a large proportion of the variation in peak force and work per cycle, but little or none of the variation in the timing of force onset or optimal contraction frequency. However, it must be kept in mind that our experiment examined the force output of muscles undergoing invariant externally imposed strain and stimulation regimes, whereas an intact animal can freely vary its strain and stimulation regime on the basis of many forms of mechanical and sensory feedback. One hypothesis is that greater muscle force should create higher wing accelerations and velocities, which should in turn cause increased wingbeat frequency. Precisely how the contractile differences that we report in the present study relate to wingbeat kinematics and aerial performance remains an open question.

We have previously presented fairly detailed discussions of the possible ecological benefits of dragonflies being able to modulate their muscle power output, flight performance and energetic costs over a wide range (Marden et al., 1998; Marden et al., 1999). Rather than repeat those arguments, which are not substantially changed by our new data, we will concentrate here on the new observation that dragonflies from different ponds show significant differences in the mean power output of their flight muscles and that morphs within ponds show different maturational trends in muscle contractile physiology. Presumably, alternative splicing of TnT is a phenotypically variable trait, which responds within individual dragonflies to changes in physical conditions (i.e. energy storage levels, frequency and intensity of flight) and social variables (i.e. crowding and the intensity of territorial interactions). Modulation of muscle contractile performance may allow dragonflies to operate at different points along a trade-off between aerial performance and energetic cost (Marden et al., 1999), and therefore it is perhaps not surprising to find that



dragonflies from different ponds have made this adjustment differently. Differences in the maturational pattern of variability in muscle contractility among morphs may reflect either different environments during the fairly distinct seasons when the two morphs are present as adults or it may reflect fixed differences in the internal hormonal environments of early- versus late-emerging dragonflies. At present, these are only hypotheses; the mechanisms and ecological ramifications of these differences among individuals, morphs and populations remain to be determined.

Many studies have examined the whole-organism functional consequences of allelic variation (Barnes and Laurie-Ahlberg, 1986; Barnes et al., 1989; Watt, 1992; Harrison et al., 1996; Powers and Schulte, 1998), but there has been little effort to date to examine how alternative splicing (i.e. non-allelic variation that arises at the RNA level) affects continuous variation in whole-organism traits. One reason for this lack of attention is that alternative splicing can be viewed as simply a mechanism for generating non-heritable phenotypic variation and is thus perhaps of little interest for population or evolutionary biology. However, our demonstration of different patterns of alternative splicing in distinct subpopulations suggests that there may be functionally important variation in the genes and pathways that control alternative splicing. Trans-regulatory genes that control alternative splicing are becoming increasingly well characterized [e.g. (Cooper, 1998; Ladd et al., 2001)], which suggests that there will be opportunities for organismal and population biologists to study these processes that amplify the complexity and phenotypic diversity obtainable from a limited number of genes.

We thank D. Grove for assistance with GENESCAN procedures and sequencing. This project was supported by NSF grants IBN-9600840, IBN-9722196 and IBN-0091040.

## References

- Baker, S. J., Sumerson, R., Reddy, C. D., Berrebi, A. S., Flynn, D. C. and Reddy, E. P. (2001). Characterization of an alternatively spliced AATYK mRNA: expression pattern of AATYK in the brain and neuronal cells. *Oncogene* **20**, 1015–1021.
- Barnes, P. T., Holland, B. and Courreges, V. (1989). Genotype-by-environment and epistatic interactions in *Drosophila melanogaster*: the effects of Gpdh allozymes, genetic background and rearing temperature on larval developmental time and viability. *Genetics* **122**, 859–868.
- Barnes, P. T. and Laurie-Ahlberg, C. C. (1986). Genetic variability of flight metabolism in *Drosophila melanogaster*. III. Effects of Gpdh allozymes and environmental temperature on power output. *Genetics* **112**, 267–294.
- Briggs, M. M., McGinnis, H. D. and Schachat, F. (1990). Transitions from fetal to fast troponin T isoforms are coordinated with changes in tropomyosin and alpha-actinin isoforms in developing rabbit skeletal muscle. *Dev. Biol.* **140**, 253–260.
- Chandra, M., Montgomery, D. E., Kim, J. J. and Solaro, R. J. (1999). The N-terminal region of troponin T is essential for the maximal activation of rat cardiac myofilaments. *J. Mol. Cell. Cardiol.* **31**, 867–880.
- Cooper, T. A. (1998). Muscle-specific splicing of a heterologous exon mediated by a single muscle-specific splicing enhancer from the cardiac troponin T gene. *Mol. Cell. Biol.* **18**, 4519–4525.
- Ewing, B. and Green, P. (2000). Analysis of expressed sequence tags indicates 35,000 human genes. *Nature Genet.* **25**, 232–234.
- Fitzhugh, G. H. and Marden, J. H. (1997). Maturational changes in troponin T expression, Ca<sup>2+</sup>-sensitivity and twitch contraction kinetics in dragonfly flight muscle. *J. Exp. Biol.* **200**, 1473–1482.
- Frey, N., Franz, W. M., Gloeckner, K., Degenhardt, M., Muller, M., Muller, O., Merz, H. and Katus, H. A. (2000). Transgenic rat hearts expressing a human cardiac troponin T deletion reveal diastolic dysfunction and ventricular arrhythmias. *Cardiovasc. Res.* **47**, 254–264.
- Harrison, J. F., Neilson, D. and Page, R. E. (1996). Malate dehydrogenase genotype, temperature and colony effects on flight metabolic rate in the honey bee, *Apis mellifera*. *Funct. Ecol.* **10**, 81–88.
- Homsher, E., Lee, D. M., Morris, C., Pavlov, D. and Tobacman, L. S. (2000). Regulation of force and unloaded sliding speed in single thin filaments: effects of regulatory proteins and calcium. *J. Physiol., Lond.* **524**, 233–243.
- Josephson, R. K. (1985). Mechanical power output from striated muscle during cyclic contraction. *J. Exp. Biol.* **114**, 493–512.
- Josephson, R. K., Malamud, J. G. and Stokes, D. R. (2000). Asynchronous muscle: a primer. *J. Exp. Biol.* **203**, 2713–2722.
- Knollmann, B. C., Blatt, S. A., Horton, K., Freitas, F. D., Miller, T. E., Bell, M., Housmans, P. R., Weissman, N. J., Morad, M. and Potter, J. D. (2001). Inotropic stimulation induces cardiac dysfunction in transgenic mice expressing a troponin T (I79N) mutation linked to familial hypertrophic cardiomyopathy. *J. Biol. Chem.* **276**, 10039–10048.
- Ladd, A. N., Charlet, N. and Cooper, T. A. (2001). The CELF family of RNA binding proteins is implicated in cell-specific and developmentally regulated alternative splicing. *Mol. Cell. Biol.* **21**, 1285–1296.
- Lopez, A. J. (1998). Alternative splicing of pre-mRNA: developmental consequences and mechanisms of regulation. *Annu. Rev. Genet.* **32**, 279–305.
- Luehrsens, K. R., Marr, L. L., Van der Knaap, E. and Cumberledge, S. (1997). Analysis of differential display RT-PCR products using fluorescent primers and GENESCAN software. *Biotechniques* **22**, 168–174.
- Lutz, G. J. and Lieber, R. L. (2000). Myosin isoforms in anuran skeletal muscle: their influence on contractile properties and *in vivo* muscle function. *Microsc. Res. Tech.* **50**, 443–457.
- Marden, J. H. (1987). Maximum lift production during takeoff in flying animals. *J. Exp. Biol.* **130**, 235–258.
- Marden, J. H. (1989). Bodybuilding dragonflies: costs and benefits of maximizing flight muscle. *Physiol. Zool.* **62**, 505–521.
- Marden, J. H. (1995). Large-scale changes in thermal sensitivity of flight performance during adult maturation in a dragonfly. *J. Exp. Biol.* **198**, 2095–2102.
- Marden, J. H., Fitzhugh, G. H. and Wolf, M. R. (1998). From molecules to mating success: integrative biology of muscle maturation in a dragonfly. *Am. Zool.* **38**, 528–545.
- Marden, J. H., Fitzhugh, G. H., Wolf, M. R., Arnold, K. D. and Rowan, B. R. (1999). Alternative splicing, muscle calcium sensitivity and the modulation of dragonfly flight performance. *Proc. Natl. Acad. Sci. USA* **96**, 15304–15309.
- Mesnard-Rouiller, L., Mercadier, J. J., Butler-Browne, G., Heimburger, M., Logeart, D., Allen, P. D. and Samson, F. (1997). Troponin T mRNA and protein isoforms in the human left ventricle: pattern of expression in failing and control hearts. *J. Mol. Cell. Cardiol.* **29**, 3043–3055.
- Miller, T., Szczesna, D., Housmans, P. R., Zhao, J., deFreitas, F., Gomes, A. V., Culbreath, L., McCue, J., Wang, Y., Xu, Y., Kerrick, W. G. and Potter, J. D. (2001). Abnormal contractile function in transgenic mice expressing an FHC-linked troponin T (179N) mutation. *J. Biol. Chem.* **276**, 3743–3755.
- Moss, R. L. (1979). Sarcomere length-tension relations of frog skinned muscle fibres during calcium activation at short lengths. *J. Physiol., Lond.* **292**, 177–192.
- Nakaura, H., Yanaga, F., Ohtsuki, I. and Morimoto, S. (1999). Effects of missense mutations Phe110Ile and Glu244Asp in human cardiac troponin T on force generation in skinned cardiac muscle fibers. *J. Biochem.* **126**, 457–460.
- Oberst, L., Zhao, G., Park, J. T., Brugada, R., Michael, L. H., Entman, M. L., Roberts, R. and Marian, A. J. (1998). Dominant-negative effect of a mutant cardiac troponin T on cardiac structure and function in transgenic mice. *J. Clin. Invest.* **102**, 1498–1505.
- Ogut, O. and Jin, J. P. (2000). Cooperative interaction between developmentally regulated troponin T and tropomyosin isoforms in the absence of F-actin. *J. Biol. Chem.* **275**, 26089–26095.
- Ohtsuki, I. (1999). Calcium ion regulation of muscle contraction: the regulatory role of troponin T. *Mol. Cell. Biochem.* **190**, 33–38.
- Pilotte, J., Larocque, D. and Richard, S. (2001). Nuclear translocation

- controlled by alternatively spliced isoforms inactivates the QUAKING apoptotic inducer. *Genes Dev.* **15**, 845–858.
- Powers, D. A. and Schulte, P. M.** (1998). Evolutionary adaptations of gene structure and expression in natural populations in relation to a changing environment: a multidisciplinary approach to address the million-year saga of a small fish. *J. Exp. Zool.* **282**, 71–94.
- Powledge, T. M.** (2000). Bear market slashes at human genome. The dropping guesses about the number of human genes challenges researchers to explain human complexity with so few genes. *EMBO Rep.* **1**, 212–214.
- Purcell, I. F., Bing, W. and Marston, S. B.** (1999). Functional analysis of human cardiac troponin by the *in vitro* motility assay: comparison of adult, foetal and failing hearts. *Cardiovasc. Res.* **43**, 884–891.
- Redwood, C., Lohmann, K., Bing, W., Esposito, G. M., Elliott, K., Abdulrazzak, H., Knott, A., Purcell, I., Marston, S. and Watkins, H.** (2000). Investigation of a truncated cardiac troponin T that causes familial hypertrophic cardiomyopathy:  $\text{Ca}^{2+}$  regulatory properties of reconstituted thin filaments depend on the ratio of mutant to wild-type protein. *Circ. Res.* **86**, 1146–1152.
- Rust, E. M., Albayya, F. P. and Metzger, J. M.** (1999). Identification of a contractile deficit in adult cardiac myocytes expressing hypertrophic cardiomyopathy-associated mutant troponin T proteins. *J. Clin. Invest.* **103**, 1459–1467.
- Simmons, P.** (1977a). The neuronal control of dragonfly flight. I. Anatomy. *J. Exp. Biol.* **71**, 123–140.
- Simmons, P.** (1977b). The neuronal control of dragonfly flight. II. Physiology. *J. Exp. Biol.* **71**, 141–155.
- Snodgrass, R. E.** (1935). *Principles of Insect Morphology*. New York: MacGraw-Hill.
- Sokal, R. R. and Rohlf, F. J.** (1995). *Biometry: the Principles and Practice of Statistics in Biological Research*. Third edition. New York: Freeman.
- Sorek, R. and Amitay, M.** (2001). Piecing together the significance of splicing. *Nature Biotech.* **19**, 196.
- Stevenson, R. D. and Josephson, R. K.** (1990). Effect of operating frequency and temperature on mechanical power output from moth flight muscle. *J. Exp. Biol.* **149**, 61–78.
- Sweeney, H. L., Feng, H. S., Yang, Z. and Watkins, H.** (1998). Functional analyses of troponin T mutations that cause hypertrophic cardiomyopathy: Insights into disease pathogenesis and troponin function. *Proc. Natl. Acad. Sci. USA* **95**, 14406–14410.
- Szathmary, E., Jordan, F. and Pal, C.** (2001). Can genes explain biological complexity? *Science* **292**, 1315–1316.
- Tardiff, J. C., Hewett, T. E., Palmer, B. M., Olsson, C., Factor, S. M., Moore, R. L., Robbins, J. and Leinwand, L. A.** (1999). Cardiac troponin T mutations result in allele-specific phenotypes in a mouse model for hypertrophic cardiomyopathy. *J. Clin. Invest.* **104**, 469–481.
- Tobacman, L. S. and Lee, R.** (1987). Isolation and functional comparison of bovine cardiac troponin T isoforms. *J. Biol. Chem.* **262**, 4059–4064.
- Wakeling, J. and Ellington, C.** (1997a). Dragonfly flight. II. Velocities, accelerations and kinematics of flapping flight. *J. Exp. Biol.* **200**, 557–582.
- Wakeling, J. and Ellington, C.** (1997b). Dragonfly flight. III. Lift and power requirements. *J. Exp. Biol.* **200**, 583–600.
- Wakeling, J. M., Cole, N. J., Kemp, K. M. and Johnston, I. A.** (2000). The biomechanics and evolutionary significance of thermal acclimation in the common carp *Cyprinus carpio*. *Am. J. Physiol.* **279**, R657–R665.
- Watkins, H., Seidman, C. E., Seidman, J. G., Feng, H. S. and Sweeney, H. L.** (1996). Expression and functional assessment of a truncated cardiac troponin T that causes hypertrophic cardiomyopathy. Evidence for a dominant negative action. *J. Clin. Invest.* **98**, 2456–2461.
- Watt, W. B.** (1992). Eggs, enzymes and evolution: natural genetic variants change insect fecundity. *Proc. Natl. Acad. Sci. USA* **89**, 10608–10612.
- Wolf, M. R.** (1999). Molecular and functional characterization of troponin T in *Libellula pulchella* and *Periplaneta americana*. PhD dissertation, Pennsylvania State University.